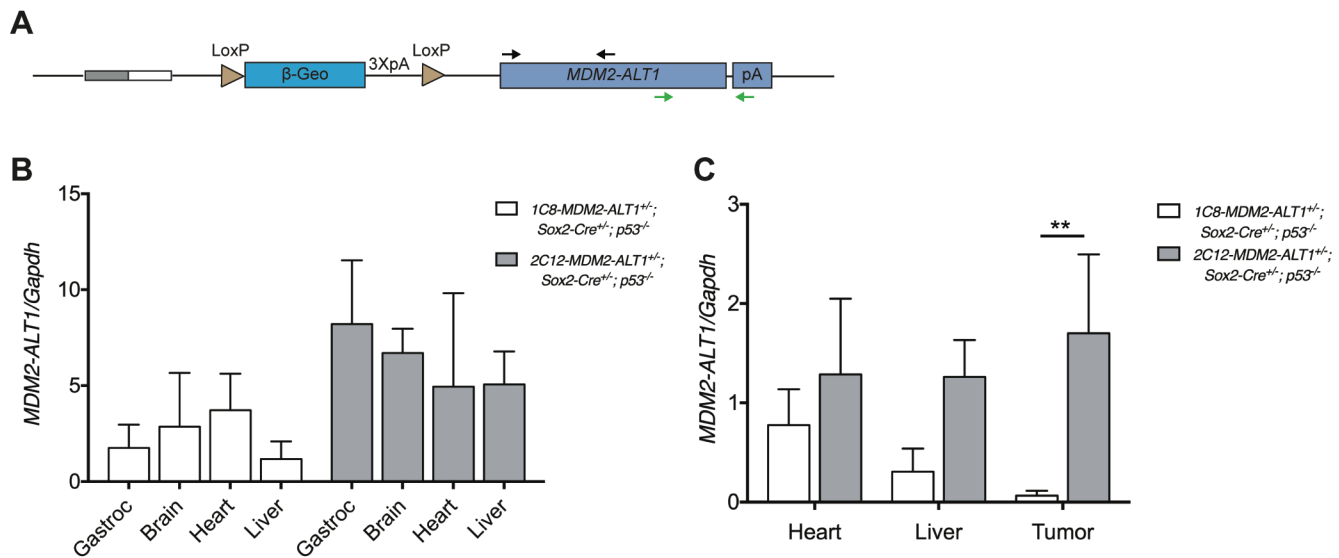
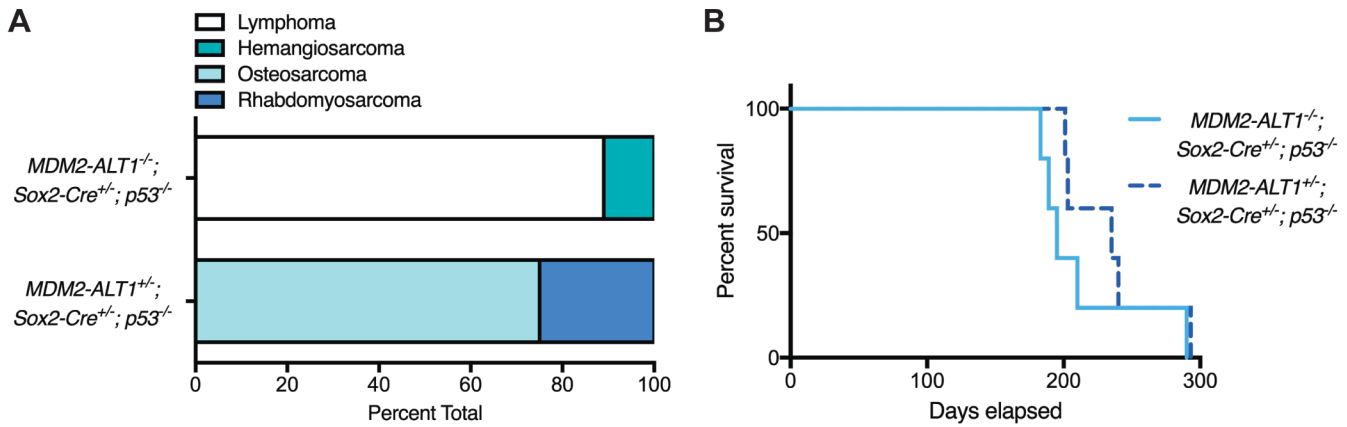


**Figure S1: MDM2-ALT1 clones display recombination in BNN132 *Escherichia coli* cells.** The pCCALL2-*MDM2-ALT1* construct was transformed into the BNN132 *Escherichia coli* strain. When the intact pCCALL2-*MDM2-ALT1* plasmid was digested with the restriction enzyme PstI, three fragments result with the following sizes (see positive control, PC lane): 7.5 kilobases, 2.8 kilobases (dark blue darts), and 118 base pairs. Recombined plasmids yield a 5.6 kilobase pairs (light blue dart) fragment upon digestion with PstI.



**Figure S2: *MDM2-ALT1* expression varies depending on tissue type and founder line.** **A.** Shown is a schematic of the integrated transgene with CMV enhancer and chicken  $\beta$ -actin promoter represented by gray and white boxes, respectively. Tan triangles signify LoxP sites and the polyadenylation signals,  $\beta$ -Geo cassette, transgene (*MDM2-ALT1*) and rabbit beta-globin polyA tail (pA) are indicated. Transgene levels were quantified using two different primer sets. One set amplified the *MDM2-ALT1* transcript in the exon 3-12 region (black arrows). A second primer set specific to the backbone of the integrated transgene amplified a region spanning exon 12 of *MDM2-ALT1* to the rabbit beta-globin polyA sequence (green arrows). **B.** Relative expression levels of the *MDM2-ALT1* transgene in tissues from experimental animals (*MDM2-ALT1*<sup>+/-</sup>; *Sox2-Cre*<sup>+/-</sup>; *p53*<sup>-/-</sup>) of both 2C12 ( $n = 2$ ) and 1C8 ( $n = 3$ ) founder lines as determined by qRT-PCR. There was no significant difference in transgene expression when comparing tissue from both founder lines and error bars represent the standard error of the mean. **C.** To avoid potential detection of mouse *Mdm2* transcripts, relative expression levels of the *MDM2-ALT1* transgene was also measured using primers specific to the integrated transgene, which spanned the 3'-end of *MDM2-ALT1* and the rabbit beta-globin polyA region. Tumors from the 2C12-*MDM2-ALT1*<sup>+/-</sup>; *Sox2-Cre*<sup>+/-</sup>; *p53*<sup>-/-</sup> ( $n = 5$ ) group had significantly higher transgene expression than 1C8-*MDM2-ALT1*<sup>+/-</sup>; *Sox2-Cre*<sup>+/-</sup>; *p53*<sup>-/-</sup> ( $n = 4$ ) mice ( $p = 0.0079$ , Mann-Whitney U test). No difference in transgene expression was detected in heart and liver tissues between experimental animals (*MDM2-ALT1*<sup>+/-</sup>; *Sox2-Cre*<sup>+/-</sup>; *p53*<sup>-/-</sup>) of 2C12 (heart  $n = 5$  and liver  $n = 3$ ) and 1C8 ( $n = 4$  for each tissue) founder lines as determined by qRT-PCR.



**Figure S3: MDM2-ALT1-expressing mice from the 1C8 founder line exhibit increased osteosarcomas compared to control mice.** **A.** Graph depicting the tumor spectrum differences between primary malignancies of the control (*MDM2-ALT1<sup>-/-</sup>; Sox2-Cre<sup>+/-</sup>; p53<sup>-/-</sup>*,  $n = 11$ ) and experimental mice (*1C8-MDM2-ALT1<sup>+/-</sup>; Sox2-Cre<sup>+/-</sup>; p53<sup>-/-</sup>*,  $n = 4$ ) as determined by a comparative pathologist. 89% of the control tumors assessed were lymphomas. However, the tumor spectrum in experimental mice showed a greater tendency for spindle cell sarcomas including osteosarcoma (75%) and rhabdomyosarcoma (25%). **B.** Kaplan-Meier curve showing that experimental mice (*1C8-MDM2-ALT1<sup>+/-</sup>; Sox2-Cre<sup>+/-</sup>; p53<sup>-/-</sup>*,  $n = 5$ ) mice show no significant difference in life span compared to mice lacking controls (*MDM2-ALT1<sup>-/-</sup>; Sox2-Cre<sup>+/-</sup>; p53<sup>-/-</sup>*,  $n = 5$ ,  $p = 0.2712$  Gehan-Breslow-Wilcoxon test).

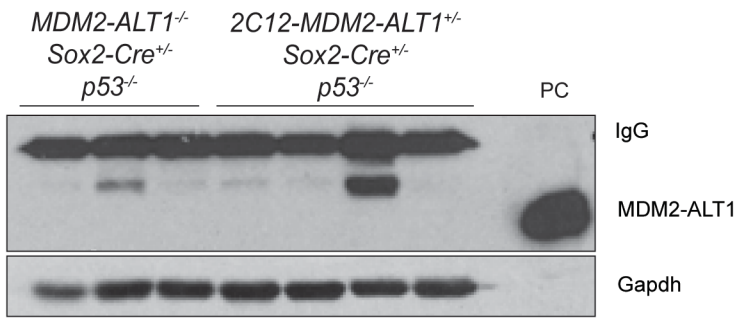


**Figure S4: MDM2-ALT1 protein expression in non-tumor tissue of experimental animals is not detected.**

Quadriceps from control (*MDM2-ALT1*<sup>-/-</sup>; *Sox2-Cre*<sup>+/-</sup>; *p53*<sup>-/-</sup>) and experimental mice (*2C12-MDM2-ALT1*<sup>+/-</sup>; *Sox2-Cre*<sup>+/-</sup>; *p53*<sup>-/-</sup>) were analyzed for protein expression of MDM2-ALT1. Detectable levels of MDM2-ALT1 protein were not observed. For comparison a positive control (PC) is shown of protein lysate from MCF7 cells transfected with a transgene containing plasmid.

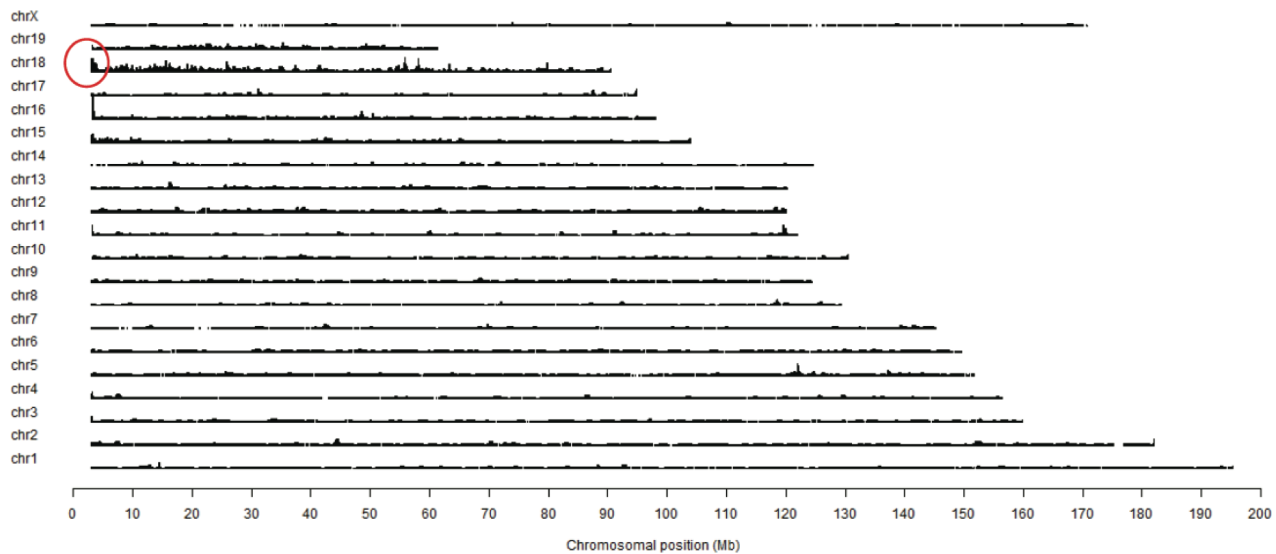


**Figure S5: The *MDM2-ALT1* transgene is integrated into mouse chromosome 18 in the 1C8 transgenic line.** Insertion site of the transgene was mapped using a TLA sequencing method for the 1C8 line. Two primer sets were used for individual TLA amplifications in the LacZ and neomycin regions. PCR products were sequenced using an Illumina sequencer. Chromosomes are indicated on the y-axis and the chromosome position on the x-axis. The highest coverage was in the centromeric region of chromosome 18 (red circle) where the transgene is inserted. Due to the site of integration, there was not a clear coverage peak in this barely annotated region of chromosome 18 and thus we cannot conclude the specific site of insertion. However, we did detect two fusions of the transgene and mouse genome indicating insertion of the 5'- and 3'-ends of the transgene into the mouse genome. Since no structural variation was detected, it is concluded that one copy of the transgene has been integrated in the mouse genome.

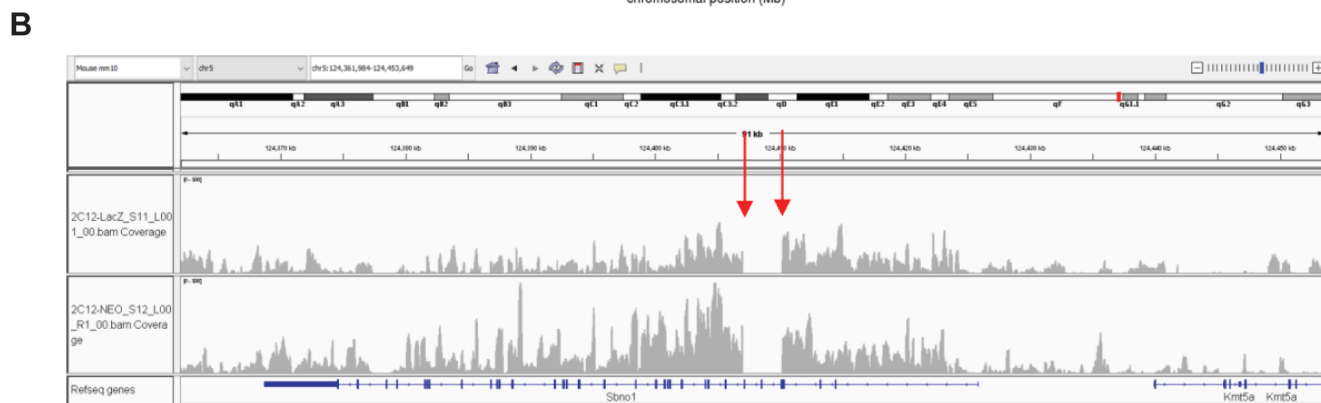
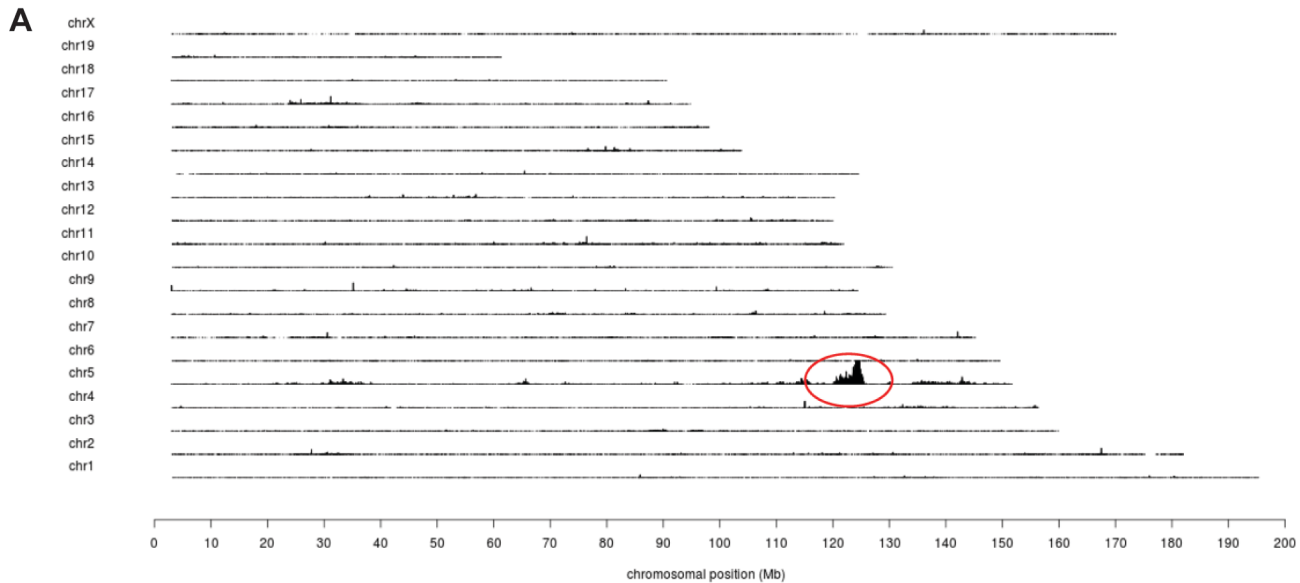


**Figure S6: The *MDM2-ALT1* transgene is integrated into mouse chromosome 5 in the 2C12 transgenic line. A.** TLA sequencing was used to map the insertion site of the transgene in the mouse genome of the 2C12 line. Two primer sets were used for individual TLA amplifications in the LacZ and Neomycin resistance regions. PCR products were sequenced using an Illumina sequencer. Chromosomes are indicated on the y-axis and the chromosome position on the x-axis. High coverage was observed on chromosome 5 (red circle), indicating transgene insertion. Good coverage was obtained for both the mouse genome and the transgene. **B.** TLA sequence coverage from both primer sets indicate the transgene was integrated in the mouse genome at chromosome 5:124,406,975 to 124,310,137 (red arrows). This region is the locus for *Sbn1* and there are no other open reading frames or identified microRNAs 50 kilobases up- or downstream of the insertion site. The site of integration includes a ~3 kb region corresponding to the gene *Sbn1*, which has been partially deleted. *Sbn1*, a strawberry notch homolog, is a protein-coding gene believed to play a role in brain and central nervous system development (1, 2). We observe no brain or central nervous system phenotypes in the *MDM2-ALT1* transgenic mice. Interestingly, *Sbn1* has been indicated to exhibit increased mutational frequency in

breast and lung cancers and is shown to be frequently mutated in the catalogue of somatic mutations in cancer database (3-5). Though these studies suggest *Sbno1* may be oncogenic in nature, there is no definitive evidence for its role in tumorigenesis. If *Sbno1* were an oncogene, its deletion would be tumor protective; however, this is not what we observe in our *2C12-MDM2-AL1<sup>+/-</sup>* cohort.

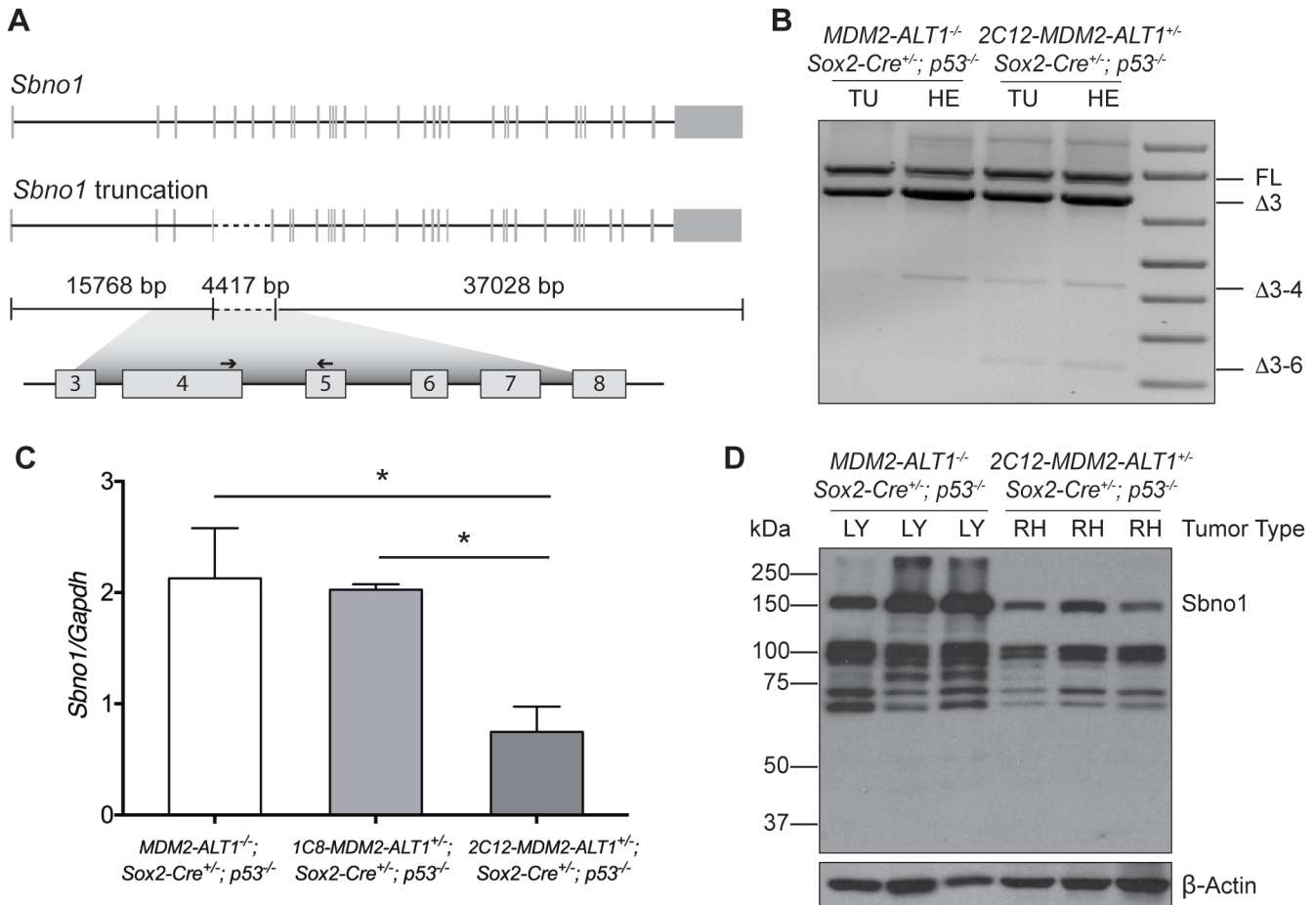


**Figure S7: Transgene integration reduces expression of *Sbno1*.** **A.** Schematic of *Sbno1* where bars indicate the 32 exons and lines represent introns. The dashed line indicates the region of *Sbno1* that was deleted as a result of transgene integration, which encompasses the last 77 nucleotides of exon 4 through the first 115 nucleotides of intron 6. Arrows indicate primers used in qPCR experiments. **B.** PCR analysis shows that the two main isoforms expressed in both control (*MDM2-ALT1<sup>-/-</sup>; Sox2-Cre<sup>+/-</sup>; p53<sup>-/-</sup>*) and experimental (*2C12-MDM2-ALT1<sup>+/-</sup>; Sox2-Cre<sup>+/-</sup>; p53<sup>-/-</sup>*) animals is the full-length isoform and one lacking exon 3 ( $\Delta 3$ ). A minor splice product is expressed lacking exons 3 and 4 ( $\Delta 3-4$ ). A transcript that lacks exons 3-6 ( $\Delta 3-6$ ) was also detected in *2C12-MDM2-ALT1<sup>+/-</sup>* animals that contains a truncated *Sbno1* allele due to transgene integration in this region, which does not correlate with a novel isoform being expressed at the protein level. **C.** To quantify transcript levels of full-length *Sbno1*, RNA was reverse transcribed from mouse livers and qPCR was performed using primers spanning exons 4-5 as indicated by arrows in **A** and only transcripts unaffected by the transgene insertion will be detected. *2C12-MDM2-ALT1<sup>+/-</sup>; Sox2-Cre<sup>+/-</sup>; p53<sup>-/-</sup>* mice ( $n = 5$ ) have significantly reduced *Sbno1* transcript expression compared to control animals *MDM2-ALT1<sup>-/-</sup>; Sox2-Cre<sup>+/-</sup>; p53<sup>-/-</sup>*;



*p53*<sup>-/-</sup> (*n* = 7, *p* = 0.037) and *1C8-MDM2-ALT1*<sup>+/-</sup>; *Sox2-Cre*<sup>+/-</sup>; *p53*<sup>-/-</sup> (*n* = 3, *p* = 0.0018, Mann Whitney U test).

**D.** In concordance with *Sbno1* transcript expression, *Sbno1* protein expression is reduced by approximately half in *2C12-MDM2-ALT1*<sup>+/-</sup> mice compared to control mice lacking the transgene. This is as expected since *2C12-MDM2-ALT1*<sup>+/-</sup> mice retain one wild-type *Sbno1* allele. Importantly, we do not observe the presence of any truncated forms of *Sbno1* protein in the tumors from mice the *2C12* line.

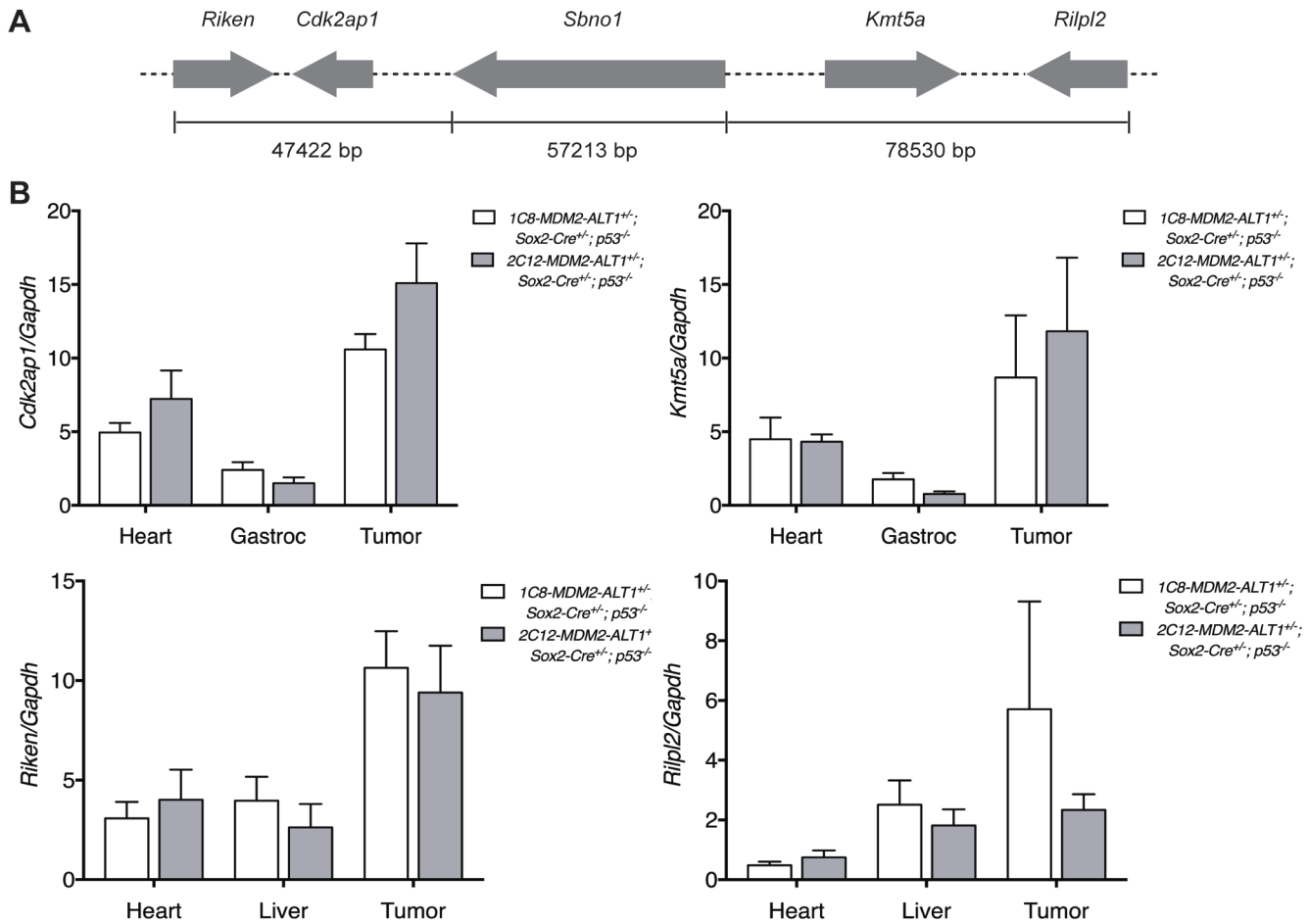


**Figure S8: MDM2-ALT1 transgene integration does not affect expression of genes surrounding *Sbno1*.**

**A.** Schematic illustration of genes near *Sbno1* where arrows represent genes and the amount of genomic space covered is indicated by basepairs listed below. **B.** qPCR was used to quantify expression of *Cdk2ap1*, *Kmt5a*, *Riken*, and *Rilpl2* in mice with transgene integrated into *Sbno1* (*2C12-MDM2-ALT1<sup>+/-</sup>; Sox2-Cre<sup>+/-</sup>; p53<sup>-/-</sup>*) or in the centromeric region of chromosome 18 (*1C8-MDM2-ALT1<sup>+/-</sup>; Sox2-Cre<sup>+/-</sup>; p53<sup>-/-</sup>*). No significant differences in transcript levels of *Cdk2ap1*, *Kmt5a*, *Riken*, or *Rilpl2* were observed in the tissues analyzed (*1C8-MDM2-ALT1<sup>+/-</sup>; Sox2-Cre<sup>+/-</sup>; p53<sup>-/-</sup>*: heart  $n = 5$  [*Cdk2ap1* and *Kmt5a*]  $n = 4$  [*Riken* and *Rilpl2*], gastroc  $n = 5$ , liver  $n = 4$ , tumor  $n = 4$ ; *2C12-MDM2-ALT1<sup>+/-</sup>; Sox2-Cre<sup>+/-</sup>; p53<sup>-/-</sup>*: heart  $n = 5$ , gastroc  $n = 4$ , liver  $n = 3$ , tumor  $n = 5$ ).

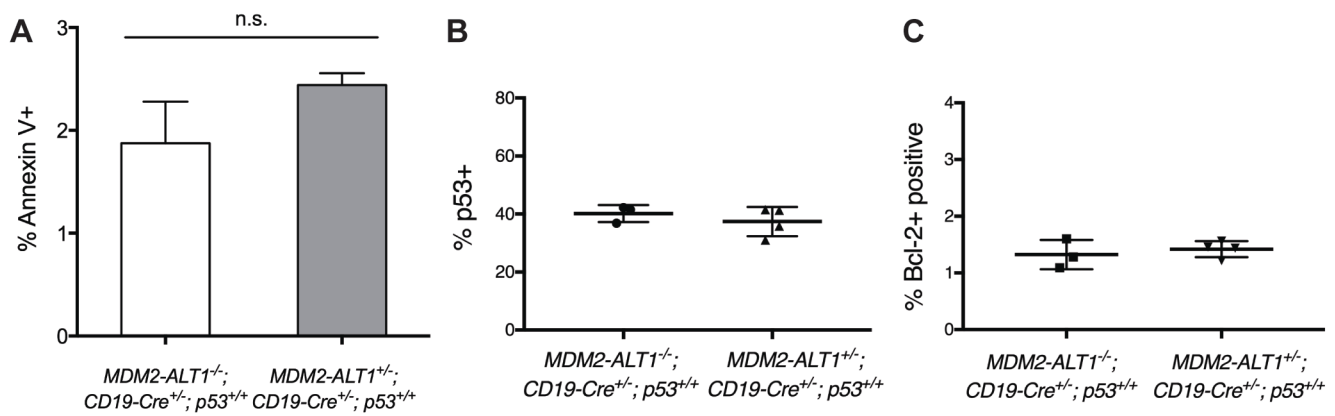


**Figure S9: B cells expressing MDM2-ALT1 display no differences in apoptosis compared to control mice.** **A.** To determine if *MDM2-ALT1* expression increases apoptosis, we collected splenocytes from both control (*MDM2-ALT1*<sup>-/-</sup>; *CD19-Cre*<sup>+/-</sup>; *p53*<sup>+/+</sup>, *n* = 6) and experimental (*2C12-MDM2-ALT1*<sup>+/-</sup>; *CD19-Cre*<sup>+/-</sup>; *p53*<sup>+/+</sup>, *n* = 7) mice four months of age and stained for B cell (B220) and T cell (CD3e) markers, as well as a live/dead discriminator. Cells were then either fixed and stained for annexin V and analyzed by flow cytometry. B cells from experimental mice showed no apparent difference in B cells undergoing apoptosis between experimental and control mice as visualized by annexin V staining. Splenocytes from 7-week old control (*MDM2-ALT1*<sup>-/-</sup>; *CD19-Cre*<sup>+/-</sup>; *p53*<sup>+/+</sup>, *n* = 3) and experimental (*2C12-MDM2-ALT1*<sup>+/-</sup>; *CD19-Cre*<sup>+/-</sup>; *p53*<sup>+/+</sup>, *n* = 4) mice were also stained for B cell markers and either p53 or Bcl2. The two cohorts showed no significant difference in cell numbers expressing p53 (**B**) or Bcl2 (**C**).

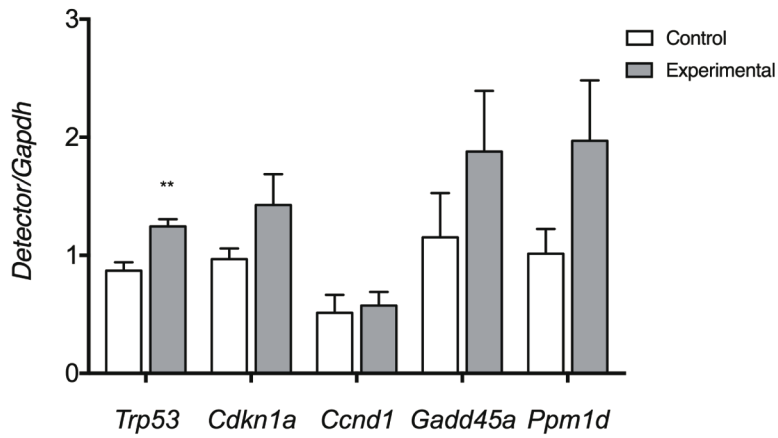


**Figure S10: Expression of *MDM2-ALT1* increases *Trp53* transcript levels.** To assess if expression of *MDM2-ALT1* affects cell cycle, we determined transcript levels of important cell cycle target genes using qPCR. RNA was reverse transcribed from spleens of control (*2C12-MDM2-ALT1*<sup>+/-</sup>; *CD19-Cre*<sup>-/-</sup>; *p53*<sup>+/+</sup> *n* = 2 and *2C12-MDM2-ALT1*<sup>-/-</sup>; *CD19-Cre*<sup>+/-</sup>; *p53*<sup>+/+</sup> *n* = 5) and experimental mice (*2C12-MDM2-ALT1*<sup>+/-</sup>; *CD19-Cre*<sup>+/-</sup>; *p53*<sup>+/+</sup> *n* = 7) 20-24 months of age. The experimental cohort expressed significantly higher levels of *Trp53* as compared to mice not expressing the transgene (*p* = 0.0082, Mann Whitney U test) whereas there was no significant difference in other cell cycle target genes.

**Table S1: Survival and malignancies of p53 null mice**

Mouse ID	Sex	Tumor type	Survival time (days)
Genotype: <i>MDM2-ALT1</i> <sup>-/-</sup> ; <i>Sox2-Cre</i> <sup>+/-</sup> ; <i>p53</i> <sup>-/-</sup>			
1031	M	lymphoma	195
1407	F	lymphoma with evidence of leukemia	191
2036	F	lymphoma; hemangiosarcoma	228
2037	F	hemangiosarcoma	213
2070	M	lymphoma	219
2088	M	lymphoma; hemangiosarcoma	214
2096	F	lymphoma with evidence of leukemia	189
2141	F	lymphoma; leiomyosarcoma	136
2161	F	lymphoma; hemangiosarcoma	138
Genotype: <i>2C12-MDM2-ALT1</i> <sup>+/-</sup> ; <i>Sox2-Cre</i> <sup>+/-</sup> ; <i>p53</i> <sup>-/-</sup>			
994	M	rhabdomyosarcoma	152
995	M	rhabdomyosarcoma	85
1044	M	lymphoma	148
1195	M	rhabdomyosarcoma; lymphoma	104
1257	M	lymphoma	53
1300	M	rhabdomyosarcoma; lymphoma	200
2039	M	rhabdomyosarcoma	145
2084	M	lymphoma with evidence of leukemia	231
2099	M	lymphoma	138
2144	M	rhabdomyosarcoma; lymphoma	70
2155	M	lymphoma	155
2158	M	teratoma; lymphoma	67

**Table S2: Survival and malignancies of p53 wild-type mice**

Mouse ID	Sex	Lymphoma sites	Additional malignancies	Age (days)
Genotype: <i>MDM2-ALT1</i> <sup>-/-</sup> ; <i>CD19-Cre</i> <sup>+/-</sup> ; <i>p53</i> <sup>+/+</sup>				
273	F	pancreatic lymph node	vulva papilloma	547
167	M	spleen	ND	547
171	F	jejunum, ileum, Peyer's patch	ND	547
226	F	spleen, mandibular lymph nodes	ND	661
241	M	mesenteric lymph node	ND	658
242	M	mesenteric lymph node	ND	658
243	F	mesenteric lymph node	ND	658
248	F	spleen, liver, omentum, adipose surrounding the mandibular SG, mediastinum, pulmonary pleura	ND	648
255	F	spleen	ND	651
259	F	spleen, Peyer's patch, inguinal lymph node	ND	637
260	F	pancreatic lymph node/omental fat, spleen, kidney, liver with evidence of leukemia	ND	637
Genotype: <i>2C12-MDM2-ALT1</i> <sup>+/-</sup> ; <i>CD19-Cre</i> <sup>+/-</sup> ; <i>p53</i> <sup>+/+</sup>				
131	F	spleen, liver, kidney, lung, vagina, harderian gland, salivary gland, lymph nodes (cervical, mediastina, pancreatic, hepatic)	tail - osteosarcoma	550
163	F	pancreatic lymph node, spleen	ND	547
168	M	pancreatic lymph node	ND	547
185	F	lymph node	ND	547
220	F	thymus, lung, kidney, liver, spleen, mandibular salivary gland, mandibular lymph nodes (mandibular, axillary, superficial, cervical, brachial, pancreatic, mesenteric)	ND	582
221	F	lymph nodes (mediastinal, gastric)	ND	582
222	M	kidneys, liver, spleen, omentum, lymph nodes (pancreatic, mandibular, axillary)	ND	582
224	M	mesenteric/pancreatic lymph node	ND	582
228	F	spleen	ND	661
230	F	Spleen and lymph nodes (inguinal, mandibular)	ND	661
236	F	mesenteric lymph node	ND	659
238	F	mesenteric lymph node	ND	659
240	F	Spleen, salivary gland, lymph nodes (mandibular, mediastinal)	ND	658
246	F	thymus, lung, pulmonary pleura -	liver - hemangioma	648
250	M	spleen	ND	648
254	F	spleen	femur hemangiosarcoma	651

269	F	thymus, pancreas, spleen, kidney, ovary, mesovarium, conjunctiva/periorcular tissues, lymph nodes (mandibular, pancreatic, gastric) with evidence of leukemia	forestomach - squamous cell carcinoma	631
270	F	spleen, lymph nodes (mandibular, pancreatic)	forestomach - squamous cell carcinoma, bone marrow - histiocytic sarcoma	640
272	F	spleen, salivary gland, lymph nodes (mandibular, axillary, mediastinal, inguinal)	ND	640

**ND: None detected**

**Table S3: Primer Table**

Primer Set	Feature	Sequences (5' - to -3')	Spanning exons
Cdk2ap1	qPCR	Sense: ATGCCCGCCGCCGCCCTCAA Antisense: CGTTCCGTTTCAGCCAAGCACTCC	Exons 1-4
Cdkn1a	qPCR	Sense: GACAAGAGGCCAGTACTTC Antisense: GCTTGGAGTGATAGAAATCTGTC	Exons 2-3
Cre	Genotyping	Sense: CCTGTTTTGCACGTTACCG Antisense: ATGCTTCTGTCCGTTTGCCG	NA
Gapdh	qPCR	Sense: AGGTCGGTGTGAACGGATTTG Antisense: TGTAGACCATGTAGTTGAGGTCA	Exons 2-3
Kmt5a	qPCR	Sense: CAGCCGGCAGAGAACCAGGATGAT Antisense: GGTGCGGGGAGACTTTCGTAGGT	Exon 8
LacZ	TLA sequencing	Sense: CTGATTCGAGGCGTTAACC Antisense: GTAGGTAGTCACGCAACTC	NA
MDM2-ALT1	qPCR	Sense: ACAAGAGACCCTGGACTAT Antisense: AAGCTTGTGTAATTTTATCATCAT	Exon junction 3/12 - Exon 12
MDM2-ALT1	Genotyping	Sense: GAGACCCTGGACTATTGG Antisense: CCCATAATTTTGGCAGAG	Exon junction 3/12 – Rabbit $\beta$ globin sequence
Neomycin	TLA sequencing	Sense: CTCCTGCCGAGAAAGTATC Antisense: TCATAGCCGAATAGCCTCT	NA
p53	Genotyping	Sense: ACAGCGTGGTGGTACCTTAT Antisense: TATACTCAGAGCCGGCCT and Sense: ACAGCGTGGTGGTACCTTAT Antisense: CTATCAGGACATAGCGTTGG	Exons 6-7  Exon 6- Neomycin insert
p53	Sequencing	Sense: TGGCCCCTGTCATCTTTTGTCC Antisense: AGGAGAGGGGGAGGCTGGTGAT	Exons 4-11
Riken	qPCR	Sense: ATGCGCAGACCTGGAAACCTTAGA Antisense: GAGCCCCACTTCCCAGAGCATA	Exons 1-2
Rilpl2	qPCR	Sense: ACCCGGCTGCAGTTCAAGATAGTA Antisense: TGCAGCACCTCCCTCAGC	Exons 1-2
Sbno1_E4-5	qPCR	Sense: CCGCCAATATTGCTCAGCCAGTTG Antisense: TTTATCCATATCCTCGCCACTTCT	Exons 4-5
Sbno1_PCR	PCR	Sense: ACCCCTACGCCCCCTTCAGTTCAA Antisense: AAGCCAGCACGGTCTCCATTAGGT	Exons 2-8
MDM2_pA	qPCR	Sense: ATAGCAGCCAAGAAGATGTGAAAG Antisense: TTGGCAGAGGGAAAAAGAT	Exon 12 - Rabbit $\beta$ globin sequence
Transgene_seq	Transgene sequencing	Sense: GCAACGTGCTGGTTATTGTG Antisense: CTAGGGGAAATAAGTTAGCACAATC	Vector backbone – Exon 12
Trp53	qPCR	Sense: CACAGCGTGGTGGTACCTTA Antisense: TCTTCTGTACGGCGGTCTCT	Exons 6-8

**NA: Not applicable**



## References

1. Takano A, Zochi R, Hibi M, Terashima T, Katsuyama Y. Expression of strawberry notch family genes during zebrafish embryogenesis. *Developmental dynamics : an official publication of the American Association of Anatomists*. 2010;239(6):1789-96.
2. Takano A, Zochi R, Hibi M, Terashima T, Katsuyama Y. Function of strawberry notch family genes in the zebrafish brain development. *The Kobe journal of medical sciences*. 2011;56(5):E220-30.
3. Sjöblom T, Jones S, Wood LD, Parsons DW, Lin J, Barber TD, et al. The Consensus Coding Sequences of Human Breast and Colorectal Cancers. *Science*. 2006;314(5797):268-74.
4. Suzuki C, Takahashi K, Hayama S, Ishikawa N, Kato T, Ito T, et al. Identification of Myc-associated protein with JmjC domain as a novel therapeutic target oncogene for lung cancer. *Molecular cancer therapeutics*. 2007;6(2):542-51.
5. Forbes SA, Beare D, Boutselakis H, Bamford S, Bindal N, Tate J, et al. COSMIC: somatic cancer genetics at high-resolution. *Nucleic Acids Research*. 2017;45(D1):D777-D83.